Food Chemistry 331 (2020) 127354

Contents lists available at ScienceDirect

Food Chemistry

journal homepage: www.elsevier.com/locate/foodchem

Liquid chromatography–mass spectrometry-based metabolomics analysis of flavonoids and anthraquinones in *Fagopyrum tataricum* L. Gaertn. (tartary buckwheat) seeds to trace morphological variations

Wei Yang[a,1], Yong Su[b,1], Gangqiang Dong[c], Guangtao Qian[b], Yuhua Shi[a], Yaolei Mi[a], Yiming Zhang[d], Jianping Xue[b], Wei Du[e], Taoxiong Shi[f], Shilin Chen[a], Yi Zhang[g], Qingfu Chen[f,*], Wei Sun[a,*]

[a] *Key Laboratory of Beijing for Identification and Safety Evaluation of Chinese Medicine, Institute of Chinese Materia Medica, China Academy of Chinese Medical Sciences, Beijing 100700, China*
[b] *College of Life Science, Huaibei Normal University, Huaibei 235000, China*
[c] *Amyway (China) Botanical R&D Centre, Wuxi 214115, China*
[d] *College of Landscape Architecture, Fujian Agriculture and Forestry University, Fuzhou 350002, China*
[e] *Agilent Technologies (China) Co., Ltd., Beijing 100102, China*
[f] *Research Center of Buckwheat Industry Technology, Guizhou Normal University, Baoshan Beilu15 116, Guiyang 550001, China*
[g] *College of Ethnic Medicine, Chengdu University of Traditional Chinese Medicine, Chengdu 611137, China*

ARTICLE INFO

Keywords:
Tartary buckwheat
Liquid chromatography–mass spectrometry
Flavonoids
Anthraquinones
Morphological variation

ABSTRACT

Polyphenols (flavonoids and anthraquinones) are one of the most important phytochemicals in *Fagopyrum tataricum* L. Gaertn. (tartary buckwheat). However, the relationship between the polyphenols of tartary buckwheat seeds and their morphological variations is unclear. We developed a liquid chromatography–mass spectrometry-based targeted metabolomics method to study the chemical profiles of 60 flavonoids and 11 anthraquinones in 40 seed cultivars (groats and hulls). Both flavonoids and anthraquinones were related to variations in seed color; the fold change from yellowish-brown to black seeds was 1.24–1.55 in groats and 0.26–0.76 in hulls. Only flavonoids contributed to significant differences in seed shape; the fold change from long to short seeds was 1.29–1.78 in groats and 1.39–1.44 in hulls. Some differential metabolites were identified at higher concentrations in hulls than in groats. This study provides new insights into differences in polyphenols among tartary buckwheat seeds with different color and shape.

1. Introduction

Fagopyrum tataricum L. Gaertn. (tartary buckwheat), an annual pseudocereal crop belonging to the Polygonaceae family, mainly grows in the mountainous regions of southwest China, northern India, Bhutan, Nepal, etc.; it has excellent agricultural significance (Cai, Corke & Li, 2004). Tartary buckwheat seeds are a type of gluten-free grains, and they comprise complete proteins with beneficial phytochemicals that protect against hypertension, fatigue, and hyperlipemia (Tsai, Deng, Tsai, & Hsu, 2012). The morphological variations in tartary buckwheat seeds are mainly reflected in two-dimensional characteristics, including differences in seed color and shape, which are important traits of plant identification and classification (Wang, Li, Zhao, & He, 2015).

Based on hull coloration and seed length, tartary buckwheat seeds can be divided into black vs. yellowish-brown and long vs. short. It is noteworthy that black tartary buckwheat (BTB) is a newly developed variety based on the traditional yellowish-brown tartary buckwheat (YTB) (Yao et al., 2017). It has been demonstrated that morphological variations in seeds are associated with their genetic, physiological, and ecological aspects involving secondary metabolites (Khan et al., 2018). To date, the correlation between edible part phenotypes and metabolic information has been reported in some plants such as wild rice and sweet potato (Wang et al., 2018; Yan et al., 2019). Chemical profile-based metabolomics approaches have been applied to distinguish

* Corresponding authors at: Institute of Chinese Materia Medica, China Academy of Chinese Medical Sciences, No.16 Nanxiaojie, Dongzhimen Nei Ave, Dongcheng District, Beijing 100700, China (W. Sun), Research Center of Buckwheat Industry Technology, Guizhou Normal University, No. 116 Baoshan Road (N), Guiyang, Guizhou 550001, China (Q. Chen).
E-mail addresses: cqf1966@163.com (Q. Chen), wsun@icmm.ac.cn (W. Sun).
[1] These authors contributed equally to this work.

https://doi.org/10.1016/j.foodchem.2020.127354
Received 14 January 2020; Received in revised form 19 May 2020; Accepted 14 June 2020
Available online 16 June 2020

cultivars, such as *Lactuca sativa*. L and *Citri Reticulatae Pericarpium*, with different morphologies (Li et al., 2019; Yang et al., 2018). However, the relationship between the secondary metabolites of tartary buckwheat seeds and their morphological variations is unclear.

Polyphenols are one of the most important phytochemicals in tartary buckwheat seeds, and they include compounds such as flavonoids and anthraquinones (Zhu, 2016). The total phenolic content in tartary buckwheat seeds is reported to be approximately 27.51–36.55 mg/g (Liu, Zhang, Zhu, & Hu, 2014). Flavonoids such as rutin, quercetin, and quercitrin have been confirmed as the main active constituents of tartary buckwheat seeds with varied biological activities, including antioxidant, antitumor, antihypertensive, and antiinflammatory activities (Kumar & Pandey, 2013). Anthraquinones such as emodin are additional important components, which are narrowly present in higher plants, especially in *Fagopyrum*, *Rheum*, *Rumex*, *Rhamnus*, *Aloe*, and the *Cassia* species. Natural anthraquinone and its derivatives exhibit antioxidant, antibacterial, and antifungal properties. To date, approximately 20 flavonoids have been isolated or identified from the seeds, leaves, buds, and flowers of tartary buckwheat (Ren, Wu, Ren, & Zhang, 2013; Kim et al., 2008; Watanabe, 1998), whereas only a few anthraquinones have been identified in tartary buckwheat seeds (Peng et al., 2013; Wu, Ge, Liang, Lv, & Sun, 2015).

Metabolomics is useful for investigating the dynamic responses of some metabolome constituents to alterations in endogenous and/or exogenous factors (Chu, Zhang, Han, & Wang, 2015; Herman et al., 2017; Wang, Alseekh, Fernie, & Luo, 2019). Monitoring of metabolic profiles using metabolomics is being increasingly applied to crop breeding for evaluating factors such as biomass, genotyping, and cross performance (Fernie & Schauer, 2009; Peluffo et al., 2010; Riedelsheimer et al., 2012; Steinfath et al., 2010). Compared with nontargeted metabolomics, targeted metabolomics is a more sensitive and accurate approach for measuring metabolites (Yang et al., 2016). However, currently available methods such as near-infrared reflectance spectroscopy (NIR) and high-performance liquid chromatography–ultraviolet spectrophotometry (HPLC–UV) that have been used for determining the multicomponents in tartary buckwheat seeds could not comprehensively explore the changes in multicomponents (Bai et al., 2015; Yang & Ren, 2008). The simultaneous use of ultraperformance liquid chromatography–triple quadrupole tandem mass spectrometry (UPLC–MS/MS) and different multiple reaction monitor (MRM) channels can allow the simultaneous quantification of multicomponents in a complex matrix (Yang et al., 2019). Therefore, a UPLC–MS/MS-based metabolomics approach using an MRM scan would be suitable for exploring the correlation between morphological variations and chemical components.

Groats produced by hulling tartary buckwheat seeds are used in the preparation of various breads, cookies, noodles, tea, and cakes; however, a substantial quantity of hulls is discarded as waste (Huang et al., 2017). Buckwheat hulls have higher antioxidant activity than buckwheat groats regardless of the cultivars; however, the comparative metabolome between hulls and groats is reportedly limited (Song, Ma, & Xiang, 2019). In the present study, we selected 40 cultivars of tartary buckwheat seeds from different regions and harvested their seeds in the same field to trace the relationship between secondary metabolites and their morphological variations using UPLC–MS/MS-based metabolomics. This analysis comprised four steps: 1) a UPLC–MS/MS-based metabolomics method was developed to study the chemical profiles of flavonoids and anthraquinones in tartary buckwheat seeds; 2) 40 tartary buckwheat seeds, which were divided into groats and hulls, with different colors and shapes were analyzed; 3) the relationships between morphological variations and secondary metabolites in tartary buckwheat groats or hulls were explored; and 4) the differences between hulls and groats of tartary buckwheat seeds were identified.

2. Material and methods

2.1. Reagents and chemicals

Epicatechin, catechin, quercetin, isoquercitrin, quercitrin, astragalin, kaempferol, rutin, and luteolin were obtained from Shanghai Yuanye Bio-Technology Co., Ltd (Shanghai, China). Chrysophanol, aloe-emodin, emodin, rhein, physcion, ω-hydroxyemodin, questinol, and emodin-8-O-β-D-glucoside were purchased from Chengdu Chroma-Biotechnology Co., Ltd. (Sichuan, China). The purity of standards was > 98%. HPLC-grade acetonitrile, methanol, acetic acid, and ammonium acetate were purchased from Thermo Fisher Scientific Inc. (Waltham, MA, USA). Ultrapure water was prepared using a Milli-Q SP system (Millipore Co., Bedford, MA, USA).

2.2. Plant materials and sample preparation

Forty cultivars of tartary buckwheat seeds were collected from Guizhou, Jiangxi, Sichuan, Yunnan, Hunan, and Gansu provinces in China in 2016 and identified using morphological and histological methods conducted by Dr. Taoxiong Shi. To exclude the influence of cultivation environment, all the cultivars were grown in April 2017 under the same environmental (experimental field of Guizhou Normal University) and soil conditions using the randomized complete block design (three rows of every accessions and three plants in each row). Mature seeds were randomly harvested from three plants, dried for 2 days in August 2017, and stored at 4 °C at the National Gene Bank of Traditional Chinese Medicine at the Institute of Chinese Materia Medica until their use for morphological and metabolomics analysis. One biological replicate was analyzed in this study. Information regarding tartary buckwheat is presented in Table 1. Parameters L* (represents lightness from black to white and from 0 to 100), a* (represents green and red seed hull color from a negative value to a positive value), and b* (represents blue and yellow seed hull color from a negative value to a positive value) regarding seed color were measured by a spectrophotometer NF555 (Nippon Denshoku Industries Co., Ltd., Japan). The length and width of the seeds were measured by a digital micrometer (Dongguan Sanliang Instrument Co., Ltd, Guangdong, China).

The tartary buckwheat seeds were crushed in a mortar to separate the hulls from groats. Then, the groats and hulls were powdered to a homogeneous size with a high-throughput tissue grinder (Shanghai Jingxin Industrial Development Co., Ltd, Shanghai, China) and sieved through a No. 50 mesh sieve. Approximately 1.0 g of sample powder was dissolved in 5.0 mL of 70% methanol aqueous in an ultrasonic ice water bath for 30 min. The solution was centrifuged at 12,000 rpm for 10 min at 4 °C and then filtered through a 0.22 μm hydrophilic organic nylon microporous membrane. Three groats and hulls samples were prepared in parallel and then mixed into one sample. All the samples were injected in a random order. In addition, eight groat powder samples and eight hull powder samples from seeds of different color and shape were used to prepare a mixed sample solution.

2.3. Preparation of standard solutions

Appropriate amounts of 14 standards were weighed and dissolved in methanol to prepare individual 1 mg/mL stock solutions. Each stock solution was mixed in methanol to prepare the quality control (QC) sample comprising 100 ng/mL rutin, isoquercitrin, quercitrin, astragalin, quercetin, epicatechin, catechin, luteolin, kaempferol, rhein, aloe-emodine, emodin, chrysophanol, and physcion. QC samples were placed in the queue for every ten experimental samples, which were used to determine “system suitability” and provide a means of monitoring the reproducibility and stability of the LC–MS system.

Table 1
The information of tartary buckwheat seeds.

No.[a]	Shape	Length/Width	Color	L*[b]	a*[c]	b*[d]	Origin
TB021	Short	1.28 ± 0.05	Yellowish-brown	34.95 ± 0.32	4.72 ± 0.34	14.58 ± 0.37	Weining, Guizhou, China
TB058	Short	1.30 ± 0.02	Yellowish-brown	34.31 ± 0.91	4.99 ± 0.12	13.69 ± 0.67	Weining, Guizhou, China
TB061	Short	1.26 ± 0.05	Yellowish-brown	39.98 ± 2.04	5.04 ± 0.68	14.95 ± 0.52	Weining, Guizhou, China
TB081	Short	1.51 ± 0.27	Yellowish-brown	33.89 ± 0.86	7.93 ± 0.38	17.33 ± 1.36	Weining, Guizhou, China
TB095	Short	1.22 ± 0.06	Yellowish-brown	31.97 ± 0.49	7.82 ± 0.21	17.27 ± 1.51	Weining, Guizhou, China
TB135	Short	1.30 ± 0.13	Yellowish-brown	32.47 ± 0.71	2.17 ± 0.97	13.78 ± 0.56	Weining, Guizhou, China
TB160	Short	1.25 ± 0.03	Yellowish-brown	30.64 ± 1.40	4.54 ± 0.70	14.19 ± 0.42	Weining, Guizhou, China
TB275	Short	1.16 ± 0.03	Yellowish-brown	31.60 ± 1.40	5.11 ± 0.68	14.96 ± 1.08	Weining, Guizhou, China
TB278	Short	1.31 ± 0.02	Yellowish-brown	33.51 ± 0.69	4.40 ± 0.64	13.99 ± 0.25	Weining, Guizhou, China
TB324	Short	1.36 ± 0.05	Yellowish-brown	34.05 ± 0.60	4.92 ± 0.36	15.53 ± 0.18	Weining, Guizhou, China
TB005	Long	1.97 ± 0.09	Yellowish-brown	37.68 ± 0.90	4.75 ± 0.40	15.93 ± 0.17	Jiujiang, Jiangxi, China
TB011	Long	2.07 ± 0.03	Yellowish-brown	30.54 ± 0.97	5.27 ± 0.88	14.21 ± 0.59	Weining, Guizhou, China
TB019	Long	1.78 ± 0.04	Yellowish-brown	30.64 ± 1.32	4.26 ± 0.40	13.17 ± 0.65	Liangshan, Sichuan, China
TB054	Long	2.04 ± 0.11	Yellowish-brown	35.56 ± 0.41	13.19 ± 0.26	20.33 ± 0.42	Nayong, Guizhou, China
TB055	Long	2.00 ± 0.16	Yellowish-brown	35.17 ± 0.29	15.79 ± 2.07	24.15 ± 1.10	Weining, Guizhou, China
TB076	Long	2.11 ± 0.03	Yellowish-brown	32.94 ± 0.36	6.19 ± 0.59	14.99 ± 0.30	Weining, Guizhou, China
TB121	Long	2.03 ± 0.06	Yellowish-brown	36.25 ± 0.97	5.20 ± 0.89	14.04 ± 0.70	Weining, Guizhou, China
TB126	Long	1.93 ± 0.05	Yellowish-brown	36.06 ± 0.42	5.19 ± 0.15	14.49 ± 0.19	Weining, Guizhou, China
TB175	Long	1.92 ± 0.04	Yellowish-brown	36.07 ± 0.49	6.04 ± 0.13	16.29 ± 0.37	Shaotong, Yunnan, China
TB180	Long	1.97 ± 0.15	Yellowish-brown	37.42 ± 0.74	6.10 ± 0.30	15.48 ± 0.33	Weining, Guizhou, China
TB098	Short	1.45 ± 0.10	Black	15.72 ± 1.89	9.16 ± 1.71	8.07 ± 1.27	Weining, Guizhou, China
TB101	Short	1.39 ± 0.06	Black	12.46 ± 1.59	5.91 ± 1.47	5.78 ± 1.88	Weining, Guizhou, China
TB115	Short	1.34 ± 0.09	Black	15.81 ± 1.11	3.38 ± 0.26	5.89 ± 0.36	Weining, Guizhou, China
TB117	Short	1.41 ± 0.20	Black	11.93 ± 1.39	4.38 ± 1.10	4.97 ± 0.74	Weining, Guizhou, China
TB165	Short	1.32 ± 0.04	Black	16.64 ± 1.05	4.72 ± 1.15	6.64 ± 1.08	Weining, Guizhou, China
TB177	Short	1.27 ± 0.10	Black	12.76 ± 0.99	4.24 ± 1.33	3.89 ± 1.14	Qujin, Yunnan, China
TB225	Short	1.32 ± 0.08	Black	14.57 ± 0.49	4.75 ± 0.26	4.73 ± 0.66	Hengyang, Hunan, China
TB291	Short	1.23 ± 0.05	Black	15.79 ± 0.21	2.79 ± 0.19	3.44 ± 0.32	Dehong, Yunnan, China
TB299	Short	1.24 ± 0.04	Black	12.60 ± 0.40	4.60 ± 0.23	5.31 ± 0.27	Weining, Guizhou, China
TB325	Short	1.32 ± 0.16	Black	14.60 ± 0.99	5.59 ± 1.39	7.09 ± 1.51	Weining, Guizhou, China
TB012	Long	1.90 ± 0.05	Black	17.65 ± 1.11	3.17 ± 1.45	6.47 ± 0.77	Dingxi, Gansu, China
TB040	Long	2.02 ± 0.16	Black	12.95 ± 0.64	2.60 ± 0.71	3.64 ± 0.16	Weining, Guizhou, China
TB063	Long	1.93 ± 0.04	Black	15.12 ± 0.63	2.52 ± 1.39	3.50 ± 0.62	Nayong, Guizhou, China
TB068	Long	1.92 ± 0.11	Black	17.07 ± 0.32	3.89 ± 0.06	4.39 ± 0.04	Xichang, Sichuan, China
TB109	Long	1.98 ± 0.07	Black	17.60 ± 1.03	2.52 ± 0.91	4.86 ± 1.39	Hezhang, Guizhou, China
TB114	Long	1.82 ± 0.02	Black	18.64 ± 0.35	5.90 ± 0.15	7.32 ± 0.08	Weining, Guizhou, China
TB128	Long	1.85 ± 0.10	Black	12.98 ± 0.41	2.22 ± 0.68	3.38 ± 1.47	Weining, Guizhou, China
TB143	Long	1.86 ± 0.06	Black	18.65 ± 0.57	3.18 ± 0.26	2.95 ± 0.14	Weining, Guizhou, China
TB190	Long	1.90 ± 0.07	Black	14.42 ± 0.34	4.80 ± 1.81	4.47 ± 0.51	Weining, Guizhou, China
TB320	Long	1.90 ± 0.05	Black	17.93 ± 0.08	3.87 ± 0.14	4.58 ± 0.25	Weining, Guizhou, China

a: number.
b: Parameter L* represents lightness: from black to white and from 0 to 100.
c: Parameter a* represents green and red from a negative value to a positive value.
d: Parameter b* represents blue and yellow from a negative value to a positive value.

2.4. Liquid chromatography–mass spectrometry conditions

The Agilent UPLC 1290II system combined with G6500 quadrupole time-of-flight mass spectrometer (QTOF) (Agilent Technologies, Santa Clara, CA, USA) was used to determine the accurate mass of metabolites. QTOF was operated using an electrospray ionization (ESI) source. Sample ionization was achieved in the positive and negative ion modes within the mass/charge (m/z) range of 100–1,000, with the following operating parameters: sheath gas temperature 350 °C, sheath gas flow 12 L/min, gas temperature 250 °C, gas flow 9 L/min, nebulizer pressure 35 psi, nozzle voltage 20 V, capillary voltage 4000 V in positive ion mode and 3,000 V in negative ion mode. The Agilent UPLC 1290II–G6400 triple quadrupole mass spectrometer (QQQ) (Agilent Technologies, Santa Clara, CA, USA) was utilized to perform MRM and product ion (PI) scans. Sample ionization was achieved in the positive and negative ion modes with the following operating parameters: sheath gas temperature 320 °C, sheath gas flow 11 L/min, gas temperature 250 °C, gas flow 7 L/min, and nebulizer pressure 30 psi. The capillary voltage in the positive and negative ion modes was set to 3,500 and 3,000 V, respectively. The MS scan functions and UPLC solvent gradients were controlled with Agilent MassHunter Workstation Software.

UPLC equipped with a binary solvent delivery system, an autosampler, and a column compartment was used. The chromatographic separations were performed on an Agilent Eclipse Plus C_{18} column (2.1 × 100 mm, 1.8 μm) with the column temperature set at 40 °C. The mobile phase A comprised water containing 0.5% acetic acid and 5 mM ammonium acetate (A) and mobile phase B comprised only acetonitrile (B), with a linear gradient elution at a flow rate of 0.3 mL/min. The gradient program was set as follows: 95% A (0–2 min); 95%–81.5% A (2–2.5 min); 81.5%–59% A (2.5–10.5 min); 59%–41% A (10.5–11 min); 41%–23% A (11–18 min); 23%–5% A (18–22 min); 5% A (22–24 min); 5%–95% A (24–24.1 min); and 95% A (24.1–26 min). The temperature of the autosampler was set at 4 °C. The volume of the sample injected was 1 μL.

2.5. Statistical analysis

Multivariate statistical analysis was performed using SIMCA-P (version 14.0, Umetrics, Umeå, Sweden), in which the orthogonal projections to latent structures–discriminant analysis (OPLS–DA) model was used to identify markers. Then, using SPSS statistics (version 16.0, SPSS Inc.), we used a t-test to analyze the differences among groups. Unless specified, a p value of < 0.05 was selected for discriminating significant differences throughout the study.

Table 2
Identification of compounds in tartary buckwheat seeds.

No.[a]	t_R[b](minute)	Parent ion(*m/z*)	Error (ppm)	Molecular formula	Molecular Mass (dalton)	Fragmentation profile (*m/z*) (Relative abundance %)	Identification
Flavonoids (flavonols, flavanols and others)							
Flavonols (parent ions: $[M+H]^+$ for compounds 1–43 except for compounds 3 and 31)							
1*	9.90	287.0550	0.03	$C_{15}H_{10}O_6$	286.0477	213.1, 153.1 (100%), 121.1	Kaempferol
2	10.50	301.0716	2.99	$C_{16}H_{12}O_6$	300.0634	286.0 (100%), 285.1, 257.9, 153.1	Isokaempferide
3*	8.24	301.0351	−1.00	$C_{15}H_{10}O_7$	302.0427	179.1, 151.1 (100%), 121.1	Quercetin
4	8.81	317.0651	−1.58	$C_{16}H_{12}O_7$	316.0583	302.1 (100%), 301.1, 273.1, 153.0, 123.1	3-O-Methylquercetin
5	10.22	317.0655	−0.32	$C_{16}H_{12}O_7$	316.0583	302.1 (100%), 285.1, 153.2	Rhamnetin
6	10.55	331.0811	−0.30	$C_{17}H_{14}O_7$	330.0740	316.1 (100%), 301.1, 273.2, 121.1	7,4′-Dimethylquercetin
7	10.83	331.0809	−0.91	$C_{17}H_{14}O_7$	330.0740	316.1, 315.1, 301.1 (100%), 273.1, 217.0, 151.1	3,5-Dimethylquercetin
8	5.49	449.1079	0.22	$C_{21}H_{20}O_{11}$	448.1006	287.0 (100%), 269.0	Kaempferol-3-O-hexoside
9	5.83	449.1074	−0.89	$C_{21}H_{20}O_{11}$	448.1006	287.0 (100%), 96.8	Kaempferol-3-O-hexoside
10*	5.92	449.1079	0.22	$C_{21}H_{20}O_{11}$	448.1006	303.1 (100%)	Quercitrin
11	6.41	449.1069	−2.00	$C_{21}H_{20}O_{11}$	448.1006	303.1 (100%)	Quercetin-O-deoxyhexoside
12	6.70	449.1079	0.22	$C_{21}H_{20}O_{11}$	448.1006	303.1 (100%)	Quercetin-O-deoxyhexoside
13	4.95	465.1034	1.29	$C_{21}H_{20}O_{12}$	464.0955	303.0 (100%),	Quercetin-3-O-hexoside
14*	5.19	465.1036	1.72	$C_{21}H_{20}O_{12}$	464.0955	303.0 (100%), 285.0, 257.1, 229.2, 165.0, 137.0	Isoquercetrin
15	6.52	465.1034	1.29	$C_{21}H_{20}O_{12}$	464.0955	303.1 (100%), 185.0, 114.1	Quercetin-O-hexoside
16	3.95	479.1178	−1.25	$C_{22}H_{22}O_{12}$	478.1111	317.0 (100%)	Methylquercetin-O-hexoside
17	4.85	479.1175	−1.88	$C_{22}H_{22}O_{12}$	478.1111	317.0 (100%), 191.0, 174.0	Methylquercetin-O-hexoside
18	5.76	479.1175	−1.88	$C_{22}H_{22}O_{12}$	478.1111	317.1 (100%), 302.1, 123.1	3-O-Methylquercetin-O-hexoside
19	6.22	479.1176	−1.67	$C_{22}H_{22}O_{12}$	478.1111	317.1 (100%)	Methylquercetin-O-hexoside
20	6.53	479.1178	−1.25	$C_{22}H_{22}O_{12}$	478.1111	317.1 (100%)	Methylquercetin-O-hexoside
21	3.97	493.1340	−0.20	$C_{23}H_{24}O_{12}$	492.1268	331.1 (100%), 316.1, 301.0, 185.1	Dimethylquercetin-O-hexoside
22	5.82	493.1345	0.81	$C_{23}H_{24}O_{12}$	492.1268	331.1 (100%)	Dimethylquercetin-O-hexoside
23	6.24	493.1347	1.22	$C_{23}H_{24}O_{12}$	492.1268	331.1 (100%), 151.1	Dimethylquercetin-O-hexoside
24	6.92	493.1340	−0.20	$C_{23}H_{24}O_{12}$	492.1268	331.1 (100%), 316.1, 301.0	Dimethylquercetin-O-hexoside
25	7.35	493.1345	0.81	$C_{23}H_{24}O_{12}$	492.1268	331.1 (100%), 121.1	Dimethylquercetin-O-hexoside
26	5.49	595.1664	1.18	$C_{27}H_{30}O_{15}$	594.1585	449.1, 287.0 (100%)	Kaempferol-3-O-hexoside deoxyhexoside
27*	4.95	611.1610	0.49	$C_{27}H_{30}O_{16}$	610.1534	465.0, 303.0 (100%)	Rutin
28	6.04	611.1604	−0.49	$C_{27}H_{30}O_{16}$	610.1534	465.0 (100%), 303.0	Quercetin-O-hexoside deoxyhexoside
29	5.61	625.1769	0.96	$C_{28}H_{32}O_{16}$	624.1690	479.1, 317.1 (100%), 301.1	Methylquercetin-O-hexoside deoxyhexoside
30	6.12	625.1770	1.12	$C_{28}H_{32}O_{16}$	624.1690	479.0, 317.0 (100%)	Methylquercetin-O-hexoside deoxyhexoside
31	8.30	623.1618	0.00	$C_{28}H_{32}O_{16}$	624.1690	299.1 (100%)	Isokaempferide-O-hexoside-hexoside
32	3.99	757.2181	−0.66	$C_{33}H_{40}O_{20}$	756.2113	611.0, 449.0 (100%), 287.0	Kaempferol-O-hexoside deoxyhexoside-O-hexoside
33	5.21	757.2177	−1.19	$C_{33}H_{40}O_{20}$	756.2113	449.0 (100%), 287.0	Kaempferol-O-hexoside deoxyhexoside-O-hexoside
34	3.88	773.2143	1.03	$C_{33}H_{40}O_{21}$	772.2062	465.0 (100%), 303.0	Quercetin-O-hexoside deoxyhexoside-O-hexoside
35	4.28	773.2137	0.26	$C_{33}H_{40}O_{21}$	772.2062	465.1, 449.1, 303.0 (100%)	Quercetin-O-hexoside deoxyhexoside-O-hexoside
36	4.44	773.2131	−0.52	$C_{33}H_{40}O_{21}$	772.2062	303.0 (100%)	Quercetin-O-hexoside deoxyhexoside-O-hexoside
37	4.73	773.2130	−0.65	$C_{33}H_{40}O_{21}$	772.2062	611.0, 465.1, 303.0 (100%)	Quercetin-O-hexoside deoxyhexoside-O-hexoside
38	5.40	773.2130	−0.65	$C_{33}H_{40}O_{21}$	772.2062	303.0 (100%)	Quercetin-O-hexoside deoxyhexoside-O-hexoside
39	5.00	893.2565	0.90	$C_{37}H_{48}O_{25}$	892.2485	747.0, 585.1, 303.0 (100%), 265.1, 121.1	Quercetin-O-hexoside deoxyhexoside-O-xylobiose
40	5.14	893.2557	0.56	$C_{37}H_{48}O_{25}$	892.2485	585.1, 303.0 (100%), 121.1	Quercetin-O-hexoside deoxyhexoside-O-xylobiose
41	6.41	893.2559	0.22	$C_{37}H_{48}O_{25}$	892.2485	585.1, 303.0 (100%)	Quercetin-O-hexoside deoxyhexoside-O-xylobiose
42	3.82	935.2667	0.43	$C_{39}H_{50}O_{26}$	934.2590	773.0, 627.0, 611.0, 465.0, 449.0, 303.0 (100%)	Quercetin-O-hexoside deoxyhexoside-O-hexoside-O-hexoside
43	3.98	935.2663	0.53	$C_{39}H_{50}O_{26}$	934.2590	627.0, 303.0 (100%)	Quercetin-O-hexoside deoxyhexoside-O-hexoside-O-hexoside
Flavanols (parent ions: $[M+H]^+$ for compounds 44–54)							
44*	4.11	291.0864	0.34	$C_{15}H_{14}O_6$	290.0790	273.1, 161.2, 147.1, 139.1 (100%), 123.1	Epicatechin
45*	4.39	291.0863	0.01	$C_{15}H_{14}O_6$	290.0790	273.1, 207.1, 165.1, 161.0, 147.0, 139.1(100%), 123.0	Catechin
46	6.57	411.1079	1.22	$C_{22}H_{18}O_8$	410.1002	273.1, 139.1 (100%), 123.1	Epicatechin/Catechin-O-hydroxybenzoate
47	6.87	411.1077	0.73	$C_{22}H_{18}O_8$	410.1002	273.1, 151.1, 139.1, 123.1 (100%)	Epicatechin/Catechin-O-hydroxybenzoate
48	7.30	411.1077	0.73	$C_{22}H_{18}O_8$	410.1002	273.1, 139.1, 123.1 (100%)	Epicatechin/Catechin-O-hydroxybenzoate
49	3.92	453.1390	−0.22	$C_{21}H_{24}O_{11}$	452.1319	291.2 (100%), 165.1, 139.1, 123.0	Epicatechin-O-hexoside
50	4.09	453.1385	−1.32	$C_{21}H_{24}O_{11}$	452.1319	291.2 (100%), 273.1, 139.1, 123.0	Catechin-O-hexoside
51	5.88	683.1755	−0.59	$C_{37}H_{30}O_{13}$	682.1686	515.0, 411.0 (100%), 393.1, 287.0, 273.1, 231.1, 151.1, 123.0	Epicatechin/catechin-O-hydroxybenzoate-O-epicatechin/catechin
52	6.17	683.1765	0.88	$C_{37}H_{30}O_{13}$	682.1686	515.0, 411.0 (100%), 393.1, 273.1, 211.1, 151.1, 123.0	Epicatechin/catechin-O-hydroxybenzoate-O-epicatechin/catechin
53	7.71	683.1759	0.66	$C_{37}H_{30}O_{13}$	682.1686	287.2, 273.1 (100%), 231.1	Epicatechin/catechin-O-hydroxybenzoate-O-epicatechin/catechin
54	8.19	683.1761	0.29	$C_{37}H_{30}O_{13}$	682.1686	273.1 (100%)	Epicatechin/catechin-O-hydroxybenzoate-O-epicatechin/catechin

(*continued on next page*)

Table 2 (*continued*)

No.[a]	t_R[b](minute)	Parent ion(*m/z*)	Error (ppm)	Molecular formula	Molecular Mass (dalton)	Fragmentation profile (*m/z*) (Relative abundance %)	Identification
Other flavonoids (parent ions: $[M+H]^+$ for compounds 55 and 58–60, $[M-H]^-$ for compound 56 and 57)							
55	8.20	273.0753	−1.46	$C_{15}H_{12}O_5$	272.0685	255.0, 137.0 (100%)	Naringenin
56*	8.17	285.0405	0.00	$C_{15}H_{10}O_6$	286.0477	229.1, 171.1, 133.0 (100%)	Luteolin
57	6.79	287.0557	−1.39	$C_{15}H_{12}O_6$	288.0634	259.0, 241.1, 125.0 (100%)	Tetrahydroxyflavanone
58	4.00	435.1284	−0.46	$C_{21}H_{22}O_{10}$	434.1213	273.1 (100%)	Naringenin-O-hexoside
59	6.93	435.1287	0.23	$C_{21}H_{22}O_{10}$	434.1213	273.1 (100%)	Naringenin-O-hexoside
60	6.02	449.1085	1.56	$C_{21}H_{20}O_{11}$	448.1006	287.0 (100%), 137.1	Cyanidin-3-O-hexoside
Anthraquinones *(parent ions: $[M-H]^-$ for compounds 61–71)*							
61*	11.97	269.0452	−1.12	$C_{15}H_{10}O_5$	270.0528	240.1(100%), 225.1	Aloe-emodin
62*	12.76	269.0451	−1.49	$C_{15}H_{10}O_5$	270.0528	241.1, 225.1 (100%)	Emodin
63	6.94	271.0242	−2.21	$C_{14}H_8O_6$	272.0321	253.0 (100%), 225.1	Tetrahydroxyanthraquinone
64	9.05	271.0243	−1.84	$C_{14}H_8O_6$	272.0321	253.1 (100%), 227.1	Tetrahydroxyanthraquinone
65*	7.35	283.0250	0.71	$C_{15}H_8O_6$	284.0321	239.1 (100%), 211.0, 183.0	Rhein
66*	12.25	283.0609	−1.06	$C_{16}H_{12}O_5$	284.0321	268.0, 240.0 (100%)	Physcion
67*	9.98	285.0405	−1.75	$C_{15}H_{10}O_6$	286.0477	267.0, 257.0, 229.0, 211.1 (100%)	ω-Hydroxyemodin
68*	7.87	299.0560	−0.33	$C_{16}H_{12}O_6$	300.0634	256.1 (100%)	Questinol
69	5.75	431.0981	−0.70	$C_{21}H_{20}O_{10}$	432.1056	269.1 (100%)	Aloe-emodin/Emodin-O-hexoside
70	6.68	431.0978	−1.39	$C_{21}H_{20}O_{10}$	432.1056	269.1 (100%)	Aloe-emodin/Emodin-O-hexoside
71*	8.40	431.0980	−0.93	$C_{21}H_{20}O_{10}$	432.1056	269.1 (100%)	Emodin-8-O-glucoside

a: number; compounds identified with standards are marked with*.
b: t_R indicates retention time.

3. Results and discussion

3.1. Identification of flavonoids and anthraquinones in tartary buckwheat seeds

We identified the compounds in tartary buckwheat seeds, i.e., the mixed samples of groats and hulls. The high-resolution full scan of UPLC–QTOF–MS determined the accurate mass of the compounds. The fragmentation profiles of the constituents were provided by a PI scan of UPLC–QQQ–MS/MS. The structures of the constituents were analyzed by matching the MS and MS/MS spectra to those of authentic standards and known literatures. Eventually, 71 compounds were identified or tentatively characterized in tartary buckwheat seeds, namely 60 flavonoids (43 flavonols, 11 flavanols, and 6 other flavonoids) and 11 anthraquinones. Their detailed information regarding their accurate mass, fragmentation ions of MS^2, and retention time is presented in Table 2.

3.1.1. Flavonoids

3.1.1.1. Flavonols. Several flavonols were isolated from the tartary buckwheat seed sample. The major flavonol glycosides comprised two types of aglycones, quercetin, and kaempferol. The sugar moieties such as glucoside, rhamnose, and rutinoside were mostly cleaved from these isolated flavonol glycosides, which corresponded to the neutral losses of 162, 146, and 308 Da, respectively. In this study, five flavonols (compounds 1, 3, 10, 14, and 27) were unambiguously identified as kaempferol, quercitrin, quercetin, isoquercetrin, and rutin, respectively, by comparing their retention times, adduct ions, and product ions with those of authentic standards.

Compound 2 was identified as isokaempferide with the molecular formula $C_{16}H_{12}O_6$, for which a series of fragment ions $[M+H\text{-}CH_3]^+$ at *m/z* 286.0 and $[M+H\text{-}CH_4]^+$ at *m/z* 285.1 and characteristic fragments of Retro Diels–Alder (RDA) reaction cleavage *m/z* 153.0 has been detected from tartary buckwheat bran (Bao, Zhou, Zhang, Peng, & Li, 2003).

Two flavonols (compounds 4 and 5) were deduced to have the molecular formula $C_{16}H_{12}O_7$. In the MS^2 spectrum, the ion at *m/z* 317.1 fragmented to an ion $[M+H\text{-}CH_3]^+$ at *m/z* 302.1 and characteristic fragments of RDA reaction cleavage *m/z* 153.0. Considering the characteristic ion $[M+H\text{-}CH_4]^+$ at *m/z* 301.1 of compound 4, compounds 4 and 5 were tentatively identified as 3-O-methylquercetin and rhamnetin, respectively, both of which have been isolated from *Fagopyrum dibotrys* (D. Don) Hara (Wu, Zhou, & Pan, 2008; Wang, Zhang, & Yang, 2005).

Compounds 6 and 7 were tentatively identified as 7,4′-dimethylquercetin and 3,5-dimethylquercetin, respectively, in agreement with ions $[M+H]^+$ at *m/z* 331.0811 and 331.0809, respectively. The MS^2 spectra of both these compounds presented fragment ions $[M+H\text{-}CH_3]^+$ at *m/z* 316.1 and $[M+H\text{-}2CH_3]^+$ at *m/z* 301.1, respectively. Compound 7 had the characteristic ion $[M+H\text{-}CH_4]^+$ at *m/z* 315.1, which has been previously identified in *Fagopyrum* dibotrys (D. Don) Hara (Wang et al., 2005).

Five flavonols (compounds 8–12) were identified with the molecular formula $C_{21}H_{20}O_{11}$. In the MS^2 spectra of compounds 8 and 9, the ion at *m/z* 449.1 was fragmented to the ion $[M+H\text{-}162\ Da]^+$ at *m/z* 287.0. Therefore, compounds 8 and 9 were tentatively identified as kaempferol-3-O-β-D-galactoside and kaempferol-3-O-β-D-glucoside, respectively, which have been previously detected in tartary buckwheat (Ren et al., 2013). In the MS^2 spectra of compounds 10–12, the ion at *m/z* 449.1 was fragmented to the ion $[M+H\text{-}146\ Da]^+$ at *m/z* 303.1, indicating loss of rhamnose, and these compounds were putatively identified as quercetin-O-rhamnoside. Compound 10 was unequivocally identified as quercitrin based on the authentic standard.

Three flavonols (compounds 13–15) were determined to have the molecular formula $C_{21}H_{20}O_{12}$, with a characteristic ion $[M+H\text{-}162\ Da]^+$ at *m/z* 303.0. Therefore, they were tentatively identified as quercetin-O-hexose. Compound 14 was unequivocally identified as isoquercetrin according to the authentic standard. The elution order of glycosylated flavonoids with a monosaccharide at the same position was galactoside > glucoside in C_{18} columns; therefore, compound 13 was identified as quercetin-3-O-β-D-galactoside, which has been previously identified in tartary buckwheat seeds (Ren et al., 2013).

Five flavonols (compounds 16–20) were determined to have the molecular formula $C_{22}H_{22}O_{12}$, with a characteristic ion $[M+H\text{-}162\ Da]^+$ at *m/z* 317.0. Therefore, compounds 16, 17, 19, and 20 were identified as methylquercetin-O-hexose; compound 18 was identified as 3-O-methylquercetin-O-hexose owing to the similar fragment ions of compound 4.

Five flavonols (compounds 21–25) with the same molecular formula $C_{23}H_{24}O_{12}$, a characteristic ion $[M+H\text{-}162\ Da]^+$ at *m/z* 331.1, and fragment ions at *m/z* 316.1 and 301.0 were presented in the MS^2 spectra of compounds 21 and 24. Therefore, compounds 21–25 were determined to be dimethylquercetin-O-hexose.

Compound 26 exhibited the deprotonated ion $[M+H]^+$ at *m/z*

595.1664. The fragment ions $[M+H\text{-}146\ Da]^+$ at *m/z* 449.1 and $[M+H\text{-}146\ Da\text{-}162\ Da]^+$ at *m/z* 287.0 were recorded in the MS/MS spectrum; therefore, it was tentatively identified as kaempferol-3-O-rutinoside, which has been previously identified in tartary buckwheat seed (Jiang et al., 2015)

Two compounds (compounds 27 and 28) were detected to have the same molecular formula $C_{27}H_{30}O_{16}$ and a series of the fragment ions at *m/z* 465.0 and 303.0. Compound 27 was unequivocally identified as rutin based on an authentic standard, whereas compound 28 was tentatively identified as quercetin-O-rutinoside.

The molecular formulas of three flavonols (compounds 29–31) were deduced to be $C_{28}H_{32}O_{16}$. Compounds 29 and 30 exhibited the adduct ion $[M+H]^+$ at *m/z* 625.1769 and 625.1770, respectively. Fragment ions $[M+H\text{-}146\ Da]^+$ at *m/z* 479.1 and $[M+H\text{-}146\ Da\text{-}162\ Da]^+$ at *m/z* 317.0 were observed in their MS/MS spectra; therefore, they were tentatively identified as methylquercetin-O-rutinoside.

Compound 31 exhibited the deprotonated ion $[M-H]^-$ at *m/z* 623.1618 and major ion $[M-H-162\ Da\text{-}162\ Da]^-$ at *m/z* 299.1 and was deduced to be isokaempferide-O-glucoside-glucoside.

Compounds 32 and 33 were tentatively identified as kaempferol-O-rutinoside-O-glucoside in agreement with the molecular formula $C_{33}H_{40}O_{20}$ and a series of the same fragment ions $[M+H\text{-}308\ Da]^+$ at *m/z* 449.0 and $[M+H\text{-}308\ Da\text{-}162\ Da]^+$ at *m/z* 287.0.

Compounds 34–38 were tentatively identified as quercetin-O-rutinoside-O-glucoside in agreement with the molecular formula $C_{33}H_{40}O_{21}$ and the same fragment ions $[M+H\text{-}308\ Da\text{-}162\ Da]^+$ at *m/z* 287.0. Among them, quercetin-3-O-rutinoside-3′-O-β-glucopyranoside has been previously identified in tartary buckwheat seeds (Jiang et al., 2015).

Compounds 39–41 ($C_{37}H_{48}O_{25}$) were tentatively identified as quercetin-O-rutinoside-O-xylobiose for a series of the same fragment ions $[M+H\text{-}308\ Da]^+$ at *m/z* 585.1 and $[M+H\text{-}308\ Da\text{-}282\ Da]^+$ at *m/z* 303.0, whereas compounds 42 and 43 ($C_{39}H_{50}O_{26}$) were temporarily recognized as quercetin-O-rutinoside-O-glucoside-O-glucoside for the same fragment ions $[M+H\text{-}308\ Da]^+$ at *m/z* 627.0 and $[M+H\text{-}308\ Da\text{-}162\ Da\text{-}162\ Da]^+$ at *m/z* 303.0.

3.1.1.2. Flavanols. In the present study, 11 flavanols were detected in tartary buckwheat seeds. Epicatechin (compound 44) and catechin (compound 45) were unequivocally identified in reference to the authentic standards. The retention time of epicatechin is consistently earlier than that of catechin.

Three flavanols (compounds 46–48) were determined to have the same molecular formula $C_{22}H_{18}O_8$. Fragment ions $[M+H\text{-}138\ Da]^+$ at *m/z* 273.1 corresponded to the loss of hydroxybenzoate. The same fragment ions at *m/z* 273.1, 139.1, and 123.1 were identified for epicatechin and catechin; therefore, these compounds were deduced as epicatechin/ catechin-O-hydroxybenzoate. According to the literature, epicatechin-3-O-hydroxybenzoate has been previously isolated from buckwheat (Watanabe, 1998).

Compounds 49 and 50 ($C_{21}H_{24}O_{11}$) were tentatively identified as epicatechin-3-O-glucoside and catechin-3-O-glucoside, respectively, sharing the same fragment ions $[M+H\text{-}162\ Da]^+$ at *m/z* 291.2 and $C_6H_3O_3^+$ at *m/z* 123.1. Epicatechin-7-O-glucoside and catechin-7-O-glucoside have been previously identified in buckwheat and tartary buckwheat, respectively (Ren et al., 2013; Watanabe, 1998).

Four flavanols (compounds 51–54) were tentatively identified as epicatechin/catechin-O-hydroxybenzoate-O-epicatechin/catechin for the same molecular formula $C_{37}H_{30}O_{13}$ and characteristic ions $[M+H\text{-}272\ Da]^+$ at *m/z* 411.0 and $[M+H\text{-}272\ Da\text{-}138\ Da]^+$ at *m/z* 273.0.

3.1.1.3. Other flavonoids. In the present study, we tentatively identified four dihydroflavonols (compounds 55, 57, 58, and 59), one flavone (compound 56), and one anthocyanidin (compound 60) in tartary buckwheat seeds. Based on the authentic standards, luteolin (compound 56) was unequivocally identified in tartary buckwheat seeds.

Compound 55 was identified as naringenin with the molecular formula $C_{15}H_{12}O_5$, fragment ion $[M+H\text{-}H_2O]^+$ at *m/z* 255.0, and the characteristic fragment of RDA cleavage at *m/z* 137.0, which has been previously isolated from other species of the Polygonaceae family, such as *Polygonum cuspidatum* (Ma et al., 2009). Compound 57 ($C_{15}H_{12}O_6$) was tentatively identified as tetrahydroxy flavanone with its fragment ions $[M-H-CO]^-$ at *m/z* 259.0 and $[M-H-H_2O]^-$ at *m/z* 241.1, whereas compounds 58 and 59 ($C_{21}H_{22}O_{10}$) were tentatively classified as naringenin-O-glucoside, cleaving the same fragment ion $[M+H\text{-}162\ Da]^+$ ay *m/z* 273.1. Compound 60 ($C_{21}H_{20}O_{11}$) was tentatively identified as cyanidin-3-O-glucoside with the characteristic fragment ions $[M+H\text{-}162\ Da]^+$ at *m/z* 287.0 and RDA cleavage at *m/z* 137.0, which has been previously identified in buckwheat sprouts (Kim et al., 2007).

3.1.2. Anthraquinones

Based on previous qualitative and quantitative analysis of anthraquinones in tartary buckwheat (Peng et al., 2013; Wu et al., 2015), we speculated that more anthraquinones exist in tartary buckwheat seeds. Seven anthraquinones (compounds 61, 62, 65–68, and 71) were unambiguously identified as aloe-emodin, emodin, rhein, physcion, ω-hydroxyemodin, questinol, and emodin-8-O-glucoside, respectively, by comparing their retention times, adduct ions, and product ions with those of authentic standards. Compounds 63 and 64 ($C_{15}H_{12}O_5$) were deduced to be tetrahydroxyanthraquinone with the same fragment ion $[M-H-H_2O]^-$ at *m/z* 253.1, whereas compounds 69 and 70 ($C_{21}H_{20}O_{10}$) were tentatively identified as aloe-emodin/emodin-O-glucoside for their same characteristic fragment ions $[M+H\text{-}162\ Da]^-$ at *m/z* 269.1.

3.2. UPLC–MS/MS-based metabolomics analysis of flavonoids and anthraquinones in tartary buckwheat seeds

The 71 compounds identified in both groats and hulls of tartary buckwheat seeds (Fig. 1) were quantitatively analyzed using an MRM scan (Sun et al., 2020; Li et al., 2019). The MRM transitions of these compounds were obtained by analyzing their fragmentation profiles and structures. For optimization of MS conditions, the MRM transitions of all compounds were investigated in both the positive and negative ion modes. Compared with that observed in the negative ion mode, we found that a higher relative intensity of ion responses was demonstrated in the positive ion mode, except for flavonoid compounds 3, 31, 56, and 57 and all the anthraquinones. The collision energy of the 71 components was optimized. UPLC conditions were optimized for achieving satisfactory chromatographic settings, including the best chromatographic separation and peak symmetry (Plazonić et al., 2009). The optimized extracted ion chromatograms (EICs) and MRM transitions of the 71 identified compounds are shown in Fig. 2. All the 71 compounds identified in the groats and hulls of different cultivars of different shape and color seeds were used in OPLS–DA.

It is well known that the technical and analytical errors must be small enough to avoid interruptions in multivariate data analysis and ensure that reliable and high-quality data are acquired with UPLC–MS/MS-based metabonomics. The line plots of the QC samples generated by principal components analysis (PCA) were plotted between standard deviations of 2SD and −2SD.

3.2.1. Difference between various colors of tartary buckwheat seeds

The coloration of tartary buckwheat seeds is critically an important discriminatory factor for their cultivars. Fortunately, our collected samples comprised cultivars of tartary buckwheat seeds including BTB seeds (n = 20) and YTB seeds (n = 20) from different locations. Information regarding the color of seeds is presented in Table 1. The L* values of BTB and YTB seeds were 11.93–18.65 and 30.54–39.98, respectively. The b* values of BTB and YTB seeds were 2.95–8.07 and

Fig. 1. Seeds, groats, and hulls of four tartary buckwheat cultivars (TB063, TB177, TB054, and TB278) with different color and shape.

13.17–24.15, respectively. Those samples provided an excellent model to evaluate the metabolic variation in both groats and hulls between BTB and YTB seeds.

Representative compounds from groats of cultivars with black or yellowish-brown hulls could be revealed by OPLS–DA. High predictability (Q_2) and strong goodness of fit (R_2X, R_2Y) of the OPLS–DA models were observed on comparing the groats of BTB and YTB seed (Q_2 = 0.694, R_2X = 0.555, R_2Y = 0.921). In the plot of OPLS–DA, the groats of BTB and YTB seeds showed clear separation (Fig. 3A). Differential metabolites, including twelve flavonoids (compounds 1, 4, 7, 9, 21, 25, 46, 47, 48, 51, 53, and 58) and three anthraquinones (compounds 62, 63, and 67), were identified using filter criteria of $p < 0.05$ and variable importance for projection (VIP) > 1. The screening results have been illustrated using volcano plots (Fig. 3B). These compounds could be used to distinguish the groats of BTB and YTB seeds. As shown in Fig. 3A, the hulls of BTB and YTB seeds also showed obvious separation on OPLS–DA (Q_2 = 0.836, R_2X = 0.563, R_2Y = 0.960). A total of 18 differential metabolites were identified using filter criteria of $p < 0.05$ and VIP > 1, namely 16 flavonoids (compounds 5, 9, 16, 19, 22, 23, 29, 37, 44, 45, 49, 56, 57, 58, 59, and 60) and two anthraquinones (compounds 64 and 69). The differential metabolites, except for compounds 9 and 58, contributed to the various colors of groats and hulls.

Both flavonoids and anthraquinones contributed to the relationship between the secondary metabolites and seed color of tartary buckwheat seeds. As shown in Fig. 3C, the concentrations of all the differential metabolites in the groats of YTB seeds were higher than those in the groats of BTB seeds, and the fold change from YTB to BTB groats was 1.24–1.55. Instead, the concentrations of all the differential metabolites in the hulls of YTB seeds were lower than those in the hulls of BTB

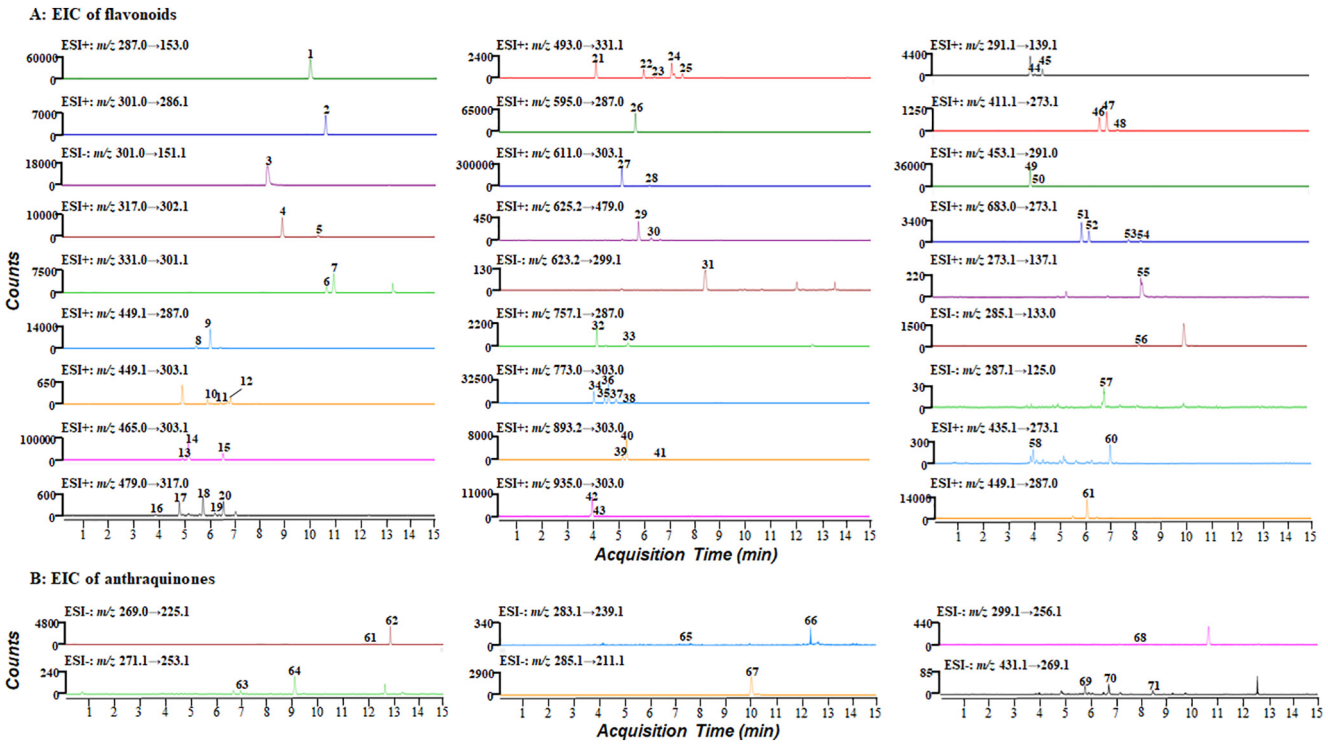

Fig. 2. The optimized extracted ion chromatograms (EIC) of the 60 flavonoids (A) and 11 anthraquinones (B) in tartary buckwheat groats (TB068). All the 71 compounds were analyzed in the positive ion mode (ESI+), except for compounds 3, 31, 56, 57, and 61–71. Compound number is consistent with the compound number in Table 2.

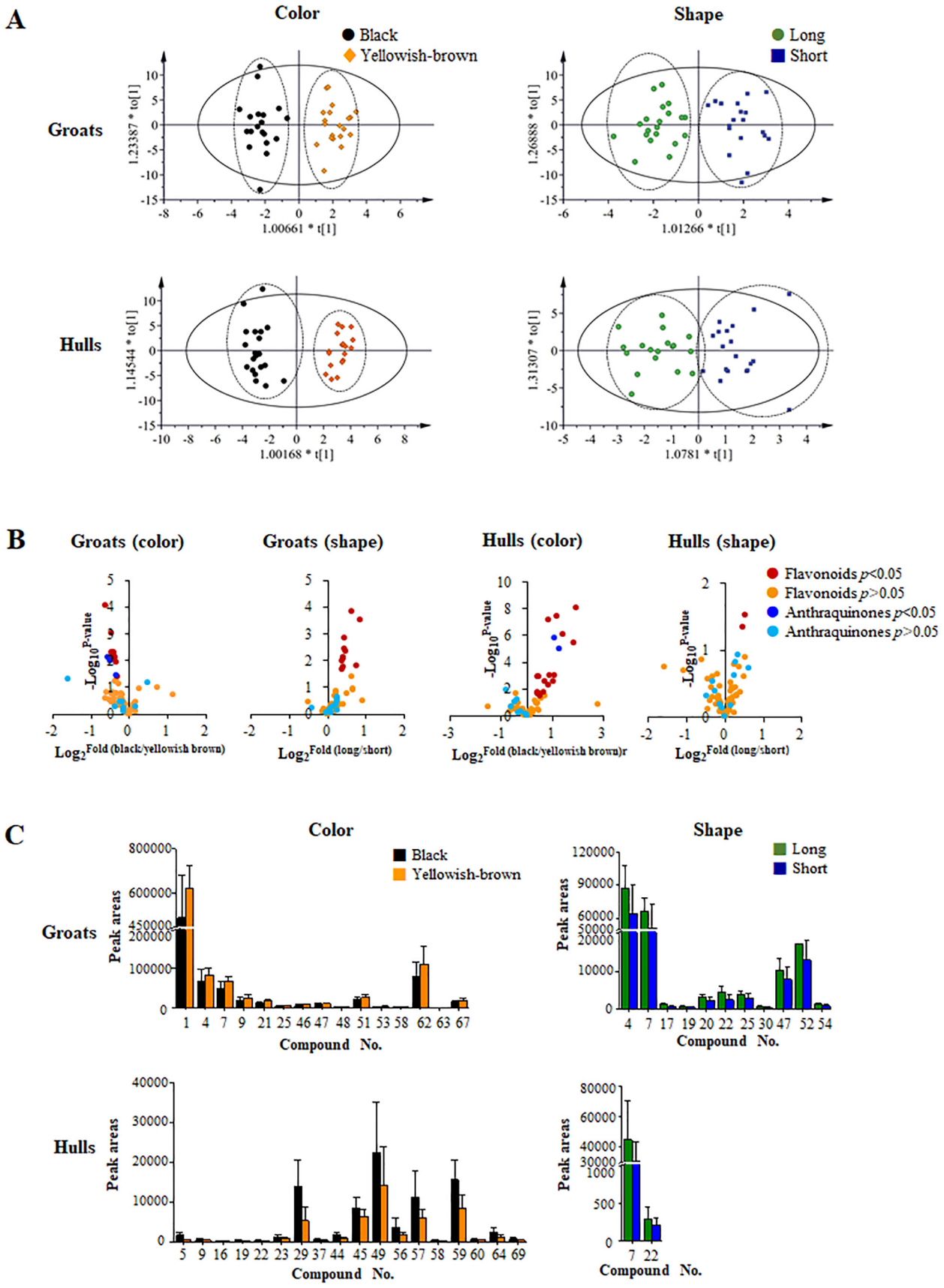

Fig. 3. Relationship between secondary metabolites (flavonoids and anthraquinones) and their morphological variations (color and shape) in tartary buckwheat seeds (groats and hulls). (A) OPLS–DA of tartary buckwheat seeds with different morphological variations; (B) Volcano plots of secondary metabolites; (C) Peak areas of differential metabolites identified in tartary buckwheat seeds with different morphological variations.

seeds. The fold change from BTB to YTB hulls was 1.32–3.78. The changing trend of differential metabolites was opposite between groats and hulls. Compared with the groats of BTB seeds, the groats of YTB seeds possibly exhibited better biological activities. To better understand the distinct features of tartary buckwheat seeds, groats and hulls should be investigated separately.

3.2.2. Difference between various shapes of tartary buckwheat seeds

The shapes of both BTB and YTB seed were simply classified into long and short, which can be determined by the length/width ratio. Our sample collection included long (n = 20) and short (n = 20) tartary buckwheat seeds, and their length/width ratio values were approximately 1.78–2.11 and 1.16–1.51, respectively (Table 1).

Good predictability (Q_2) and strong goodness of fit (R_2X, R_2Y) of the OPLS–DA models were observed in the comparison between the long and short shapes of groats (Q_2 = 0.552, R_2X = 0.590, R_2Y = 0.893). Long and short groats showed clear separation in OPLS–DA, indicating significant differences in various groat shapes (Fig. 3A). A total of 11 flavonoids (compounds 4, 7, 17, 19, 20, 22, 25, 30, 47, 52, and 54) were identified with $p < 0.05$ and VIP > 1 (Fig. 3B). As shown in Fig. 3A, the segregation between the long and short shapes of hulls was not clear in OPLS–DA (Q_2 = 0.368, R_2X = 0.467, R_2Y = 0.756), and only two flavonoids (compounds 7 and 22) were identified with statistical significance (Fig. 3B).

No significant difference was observed among anthraquinones in terms of the relationship between the secondary metabolites and shape of tartary buckwheat seeds. The concentrations of all the differential metabolites in the groats of long seeds were higher than those in in the groats of short seeds, and their fold change was 1.29–1.78 (Fig. 3C). The concentrations of these two flavonoids (compounds 7 and 22) were also higher in the hulls of long seeds than those in the hulls of short seeds, and their fold change was 1.39–1.44 (Fig. 3C). The change trend of differential metabolites in groats and hulls was consistent. Therefore, it is suggested that long seeds could have better biological activities than short ones.

3.2.3. Difference between hulls and groats of tartary buckwheat seeds

The data of the 71 compounds identified in the 40 groats and 40 hulls were used to identify differential metabolites between groats and hulls. Regardless of morphological variations, groats and hulls were well distinguished in OPLS–DA (Q_2 = 0.934, R_2X = 0.982, R_2Y = 0.956), as shown in Fig. 4A. A total of 64 different metabolites were identified with $p < 0.05$ and VIP > 1, namely 53 flavonoids and 11 anthraquinones (Fig. 4B). These metabolites can be assigned to two groups based on their change fold trends, as shown in volcano plots (Fig. 4B). We found that 17 compounds were present at higher concentrations in hulls (Fig. 4C) and 46 compounds were present at higher concentrations in groats (Fig. 4D). It is noteworthy that the concentration of rutin (a major component of tartary buckwheat) was higher in hulls than in groats, and the change fold was approximately twice more than that in groats. Nine flavonoids (compounds 2, 4, 6, 13, 27, 29, 56, 57, and 59) and eight anthraquinones (compounds 61, 64–66, and 68–71) identified in hulls were present at higher content than that observed in groats; the fold change was 1.36–29.05. It has been reported that buckwheat hulls have higher antioxidant activity than buckwheat groats regardless of the cultivars (Dziadek & Kopeć, A., Pastucha, E., Pia̧tkowska, E., Leszczyńska, T., Pisulewska, E., Witkowicz, R., & Francik, R. , 2016). Therefore, hulls should not be discarded. The utilization of tartary buckwheat hulls as feedstock could not only reduce environmental pollution but also increase the additional value of tartary buckwheat seeds.

Regarding the contribution of differential metabolites to the various colors of groats, all the 15 metabolites, except for compound 4, were present at higher concentrations in groats than in hulls. Among the 18 differential metabolites that contributed to the various colors of hulls, the concentrations of six metabolites (compounds 29, 56, 57, 59, 64, and 69) were higher in hulls than in groats. Regarding the 11 differential metabolites that contributed to the various shapes of groats, 9 metabolites (compounds 7, 17, 19, 22, 25, 30, 47, 52, and 54) were present at higher concentrations in groats. Two differential metabolites (compounds 7 and 22) that contributed to the various shapes of hulls were present at higher concentrations in groats. The findings of the present study could be used to select and breed specific compositions of tartary buckwheat seeds, which was possible by monitoring the variations in metabolomics among different cultivars.

4. Conclusion

An LC–MS/MS-based target metabolomics method was developed to study the chemical profiles of 60 flavonoids and 11 anthraquinones in tartary buckwheat seeds. This method was used to study 40 cultivars of tartary buckwheat seeds from different regions. Both flavonoids and anthraquinones contributed to the relationship between the secondary metabolites and color of tartary buckwheat seeds. However, the changing trend of differential metabolites was different between groats and hulls. Regarding the relationship between the secondary metabolites and shape of tartary buckwheat seeds, only flavonoids contributed to a significant difference. The changing trend of differential metabolites in groats and hulls was consistent. Meanwhile, different metabolites in hulls and groats of tartary buckwheat were explored. This research provides reference for the selection of tartary buckwheat seeds with optimized metabolic profiles for the precise breeding of new cultivars and also aids in assessing metabolic quality.

CRediT authorship contribution statement

Wei Yang: Supervision, Investigation, Writing - original draft, Writing - review & editing, Methodology. **Yong Su:** Supervision, Investigation, Writing - original draft, Methodology. **Gangqiang Dong:** Investigation. **Guangtao Qian:** Data curation, Formal analysis. **Yuhua Shi:** Writing - review & editing. **Yaolei Mi:** Writing - review & editing. **Yiming Zhang:** Visualization. **Jianping Xue:** Investigation. **Wei Du:** Methodology. **Taoxiong Shi:** Resources. **Shilin Chen:** Supervision. **Yi Zhang:** Supervision. **Qingfu Chen:** Writing - review & editing, Resources. **Wei Sun:** Writing - review & editing, Supervision.

Declaration of Competing Interest

The authors declare that they have no known competing financial interests or personal relationships that could have appeared to influence the work reported in this paper.

Acknowledgements

This work was supported by the opening project of State Key Laboratory of Tree Genetics and Breeding and the Fundamental Research Funds for the Central public welfare research institutes [grant numbers ZZ13-YQ-045, ZZ13-YQ-053, ZXKT19019, ZZ13-YQ-101]; National Natural Science Foundation of China [grant number 31860408]; and National Science and Technology Major Project “Creation of Major New Drugs” [grant number 2019ZX09201005-006-004].

Appendix A. Supplementary data

Region information of tartary buckwheat seeds, total ion chromatograms of seeds, collision energy information of the 71 compounds, and line plots of the quality control samples generated by principal components analysis were provided in the supplementary material. Supplementary data to this article can be found online at https://doi.org/10.1016/j.foodchem.2020.127354.

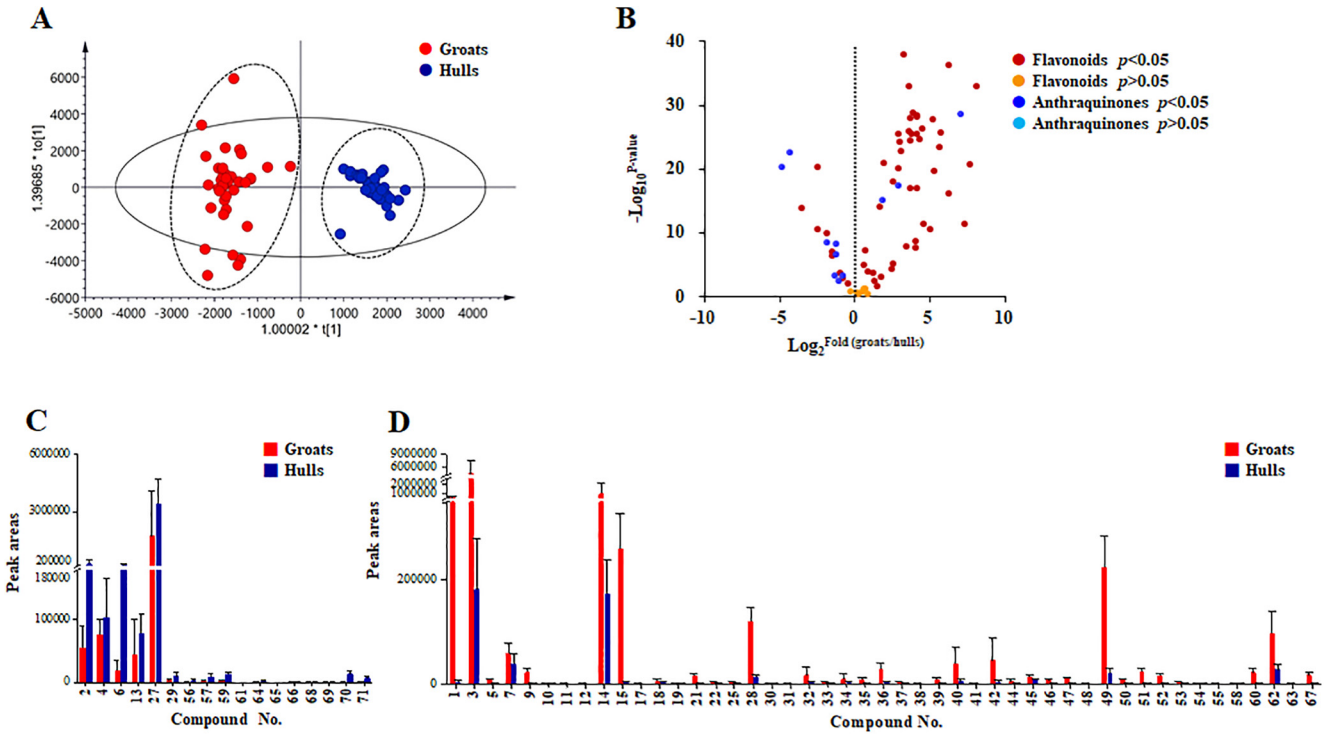

Fig. 4. Chemical differences between groats and hulls. (A) Scores plot of OPLS–DA; (B) Volcano plots; (C) Peak areas of differential metabolites that are present at higher concentrations in hulls than in groats; (D) Peak areas of differential metabolites that are present at higher concentrations in groats than in hulls.

References

Bai, C. Z., Feng, M. L., Hao, X. L., Zhong, Q. M., Tong, L. G., & Wang, Z. H. (2015). Rutin, quercetin, and free amino acid analysis in buckwheat (Fagopyrum) seeds from different locations. *Genetics and Molecular Research, 14*(4), 19040–19048. https://doi.org/10.4238/2015.December.29.11.

Bao, T. N., Zhou, Z. Z., Zhang, F., Peng, S. L., & Li, B. G. (2003). Chemical constituents from tartary buckwheat bran. *Natural Product Research and Development, 15*, 116–117. https://doi.org/10.16333/j.1001-6880.2003.01.008.

Cai, Y. Z., Corke, H., & Li, W. D. (2004). BUCKWHEAT: Elsevier.

Chu, H., Zhang, A. H., Han, Y., & Wang, X. J. (2015). *World Journal of Traditional Chinese Medicine, 1*(4), 26–32. https://doi.org/10.15806/j.issn.2311-8571.2015.0022.

Dziadek, K., Kopeć, A., Pastucha, E., Piątkowska, E., Leszczyńska, T., Pisulewska, E., ... Francik, R. (2016). Basic chemical composition and bioactive compounds content in selected cultivars of buckwheat whole seeds, dehulled seeds and hulls. *Journal of Cereal Science, 69*, 1–8. https://doi.org/10.1016/j.jcs.2016.02.004.

Fernie, A. R., & Schauer, N. (2009). Metabolomics-assisted breeding: A viable option for crop improvement? *Trends in Genetics, 25*(1), 39–48. https://doi.org/10.1016/j.tig.2008.10.010.

Herman, S., Emami, K. P., Aftab, O., Krishnan, S., Strombom, E., Larsson, R., ... Gustafsson, M. (2017). Mass spectrometry based metabolomics for in vitro systems pharmacology: Pitfalls, challenges, and computational solutions. *Metabolomics, 13*(7), 79. https://doi.org/10.1007/s11306-017-1213-z.

Huang, Y., Feng, F., Jiang, J., Qiao, Y., Wu, T., Voglmeir, J., & Chen, Z. G. (2017). Green and efficient extraction of rutin from tartary buckwheat hull by using natural deep eutectic solvents. *Food Chemistry, 221*, 1400–1405. https://doi.org/10.1016/j.foodchem.2016.11.013.

Li, C., Zang, C., Nie, Q., Yang, B., Zhang, B., & Duan, S. (2019). Simultaneous determination of seven flavonoids, two phenolic acids and two cholesterines in Tanreqing injection by UHPLC-MS/MS. *Journal of Pharmaceutical and Biomedical Analysis, 163*, 105–112. https://doi.org/10.1016/j.jpba.2018.08.058.

Liu, Q., Zhang, W., Zhu, Y., & Hu, Q. (2014). Comparison of the constitutions, distribution, and antioxidant activities of polyphenols from different varieties of tartary buckwheat seed produced from different regions of china. *Scientia Agricultura Sinica, 47*, 2840–2852. https://doi.org/10.3864/j.issn.0578-1752.2014.14.014.

Tsai, H., Deng, H., Tsai, S., & Hsu, Y. (2012). Bioactivity comparison of extracts from various parts of common and tartary buckwheats: Evaluation of the antioxidant- and angiotensin-converting enzyme inhibitory activities. *Chemistry Central Journal, 6*(1), https://doi.org/10.1186/1752-153X-6-78.

Jiang, S., Liu, Q., Xie, Y., Zeng, H., Zhang, L., Jiang, X., & Chen, X. (2015). Separation of five flavonoids from tartary buckwheat (Fagopyrum tataricum (L.) Gaertn) grains via off-line two dimensional high-speed counter-current chromatography. *Food Chemistry, 186*, 153–159. https://doi.org/10.1016/j.foodchem.2014.08.120.

Khan, W. A., Hou, X., Han, K., Khan, N., Dong, H., Saqib, M., ... Hu, C. (2018). Lipidomic study reveals the effect of morphological variation and other metabolite interactions on the lipid composition in various cultivars of Bok choy. *Biochemical and Biophysical Research Communications, 506*(3), 755–764. https://doi.org/10.1016/j.bbrc.2018.04.112.

Kim, S. J., Maeda, T., Sarker, M. Z., Takigawa, S., Matsuura-Endo, C., Yamauchi, H., ... Suzuki, T. (2007). Identification of anthocyanins in the sprouts of buckwheat. *Journal of Agricultural and Food Chemistry, 55*(15), 6314–6318. https://doi.org/10.1021/jf0704716.

Kim, S. J., Zaidul, I. S. M., Suzuki, T., Mukasa, Y., Hashimoto, N., Takigawa, S., ... Yamauchi, H. (2008). Comparison of phenolic compositions between common and tartary buckwheat (Fagopyrum) sprouts. *Food Chemistry, 110*(4), 814–820. https://doi.org/10.1016/j.foodchem.2008.02.050.

Kumar, S., & Pandey, A. K. (2013). Chemistry and biological activities of flavonoids: An overview. *Scientific World Journal, 2013*, 162750. https://doi.org/10.1155/2013/162750.

Li, S. Z., Zeng, S. L., Wu, Y., Zheng, G. D., Chu, C., Yin, Q., ... Liu, E. H. (2019). Cultivar differentiation of Citri Reticulatae Pericarpium by a combination of hierarchical three-step filtering metabolomics analysis, DNA barcoding and electronic nose. *Analytica Chimica Acta, 1056*, 62–69. https://doi.org/10.1016/j.aca.2019.01.004.

Ma, L. Q., Guo, Y. Wu., Gao, D. Y., Ma, D. M., Wang, Y. N., Li, G. F., ... Ye, H. C. (2009). Identification of a Polygonum cuspidatum three-intron gene encoding a type III polyketide synthase producing both naringenin and p-hydroxybenzalacetone. *Planta, 229*(5), 1077–1086. https://doi.org/10.1007/s00425-009-0899-1.

Peluffo, L., Lia, V., Troglia, C., Maringolo, C., Norma, P., Escande, A., ... Carrari, F. (2010). Metabolic profiles of sunflower genotypes with contrasting response to Sclerotinia sclerotiorum infection. *Phytochemistry, 71*(1), 70–80. https://doi.org/10.1016/j.phytochem.2009.09.018.

Peng, L. X., Wang, J. B., Hu, L. X., Zhao, J. L., Xiang, D. B., Zou, L., & Zhao, G. (2013). Rapid and simple method for the determination of emodin in tartary buckwheat (Fagopyrum tataricum) by high-performance liquid chromatography coupled to a diode array detector. *Journal of Agricultural and Food Chemistry, 61*(4), 854–857. https://doi.org/10.1021/jf304804c.

Ren, Q., Wu, C., Ren, Y., & Zhang, J. (2013). Characterization and identification of the chemical constituents from tartary buckwheat (Fagopyrum tataricum Gaertn) by high performance liquid chromatography/photodiode array detector/linear ion trap FTICR hybrid mass spectrometry. *Food Chemistry, 136*(3–4), 1377–1389. https://doi.org/10.1016/j.foodchem.2012.09.052.

Riedelsheimer, C., Czedik-Eysenberg, A., Grieder, C., Lisec, J., Technow, F., Sulpice, R., ... Melchinger, A. E. (2012). Genomic and metabolic prediction of complex heterotic traits in hybrid maize. *Nature Genetics, 44*(2), 217–220. https://doi.org/10.1038/ng.1033.

Plazonić, A., Bucar, F., Maleš, Z., Mornar, A., Nigović, B., & Kujundžić, N. (2009). Identification and Quantification of Flavonoids and Phenolic Acids in Burr Parsley (Caucalis platycarpos L.), Using High-Performance Liquid Chromatography with Diode Array Detection and Electrospray Ionization Mass Spectrometry. *Molecules, 14*, 2466–2490. https://doi.org/10.3390/molecules14072466.

Song, C., Ma, C., & Xiang, D. (2019). Variations in Accumulation of Lignin and Cellulose and Metabolic Changes in Seed Hull Provide Insight into Dehulling Characteristic of Tartary Buckwheat Seeds. *International Journal of Molecular Sciences, 20*(3), https://

doi.org/10.3390/ijms20030524.
Steinfath, M., Strehmel, N., Peters, R., Schauer, N., Groth, D., Hummel, J., ... Van Dongen, J. T. (2010). Discovering plant metabolic biomarkers for phenotype prediction using an untargeted approach. *Plant Biotechnology Journal, 8*(8), 900–911. https://doi.org/10.1111/j.1467-7652.2010.00516.x.
Sun, Y., Feng, G., Zheng, Y., Liu, S., Zhang, Y., Pi, Z., ... Liu, Z. (2020). Putative multiple reaction monitoring strategy for the comparative pharmacokinetics of postoral administration Renshen-Yuanzhi compatibility through liquid chromatography-tandem mass spectrometry. *Journal of Ginseng Research, 44*(1), 105–114. https://doi.org/10.1016/j.jgr.2018.09.007.
Wang, A., Li, R., Ren, L., Gao, X., Zhang, Y., Ma, Z., ... Luo, Y. (2018). A comparative metabolomics study of flavonoids in sweet potato with different flesh colors (Ipomoea batatas (L.) Lam). *Food Chemistry, 260*, 124–134. https://doi.org/10.1016/j.foodchem.2018.03.125.
Wang, K. J., Zhang, Y. J., & Yang, C. R. (2005). Antioxidant phenolic constituents from Fagopyrum dibotrys. *Journal of Ethnopharmacology, 99*(2), 259–264. https://doi.org/10.1016/j.jep.2005.02.029.
Wang, L., Li, J., Zhao, J., & He, C. (2015). Evolutionary developmental genetics of fruit morphological variation within the Solanaceae. *Frontiers in Plant Science, 6*, 248. https://doi.org/10.3389/fpls.2015.00248.
Wang, S., Alseekh, S., Fernie, A. R., & Luo, J. (2019). The Structure and Function of Major Plant Metabolite Modifications. *Molecular plant, 12*(7), 899–919. https://doi.org/10.1016/j.molp.2019.06.001.
Watanabe, M. (1998). Catechins as antioxidants from buckwheat (Fagopyrum esculentum Moench) groats. *Journal of Agricultural and Food Chemistry, 46*. https://doi.org/10.1021/jf9707546.
Wu, H. Z., Zhou, J. Y., & Pan, H. L. (2008). Study on chemical constituents of Fagopyrum dibotrys (D.Don). *Hara. Chinese Journal of Hospital Pharmacy, 28*(21), 1830–1831.
Wu, X., Ge, X., Liang, S., Lv, Y., & Sun, H. (2015). A novel selective accelerated solvent extraction for effective separation and rapid simultaneous determination of six anthraquinones in tartary buckwheat and its products by UPLC–DAD. *Food Analytical Methods, 8*(5), 1124–1132. https://doi.org/10.1007/s12161-014-9976-6.
Yan, N., Du, Y., Liu, X., Chu, M., Shi, J., Zhang, H., ... Zhang, Z. (2019). A comparative UHPLC-QqQ-MS-based metabolomics approach for evaluating Chinese and North American wild rice. *Food Chemistry, 275*, 618–627. https://doi.org/10.1016/j.foodchem.2018.09.153.
Yang, M., Yu, Z., Deng, S., Chen, X., Chen, L., Guo, Z., ... Liang, F. (2016). A Targeted Metabolomics MRM-MS Study on Identifying Potential Hypertension Biomarkers in Human Plasma and Evaluating Acupuncture Effects. *Scientific Reports, 6*, 25871. https://doi.org/10.1038/srep25871.
Yang, N., & Ren, G. (2008). Application of near-infrared reflectance spectroscopy to the evaluation of rutin and D-chiro-Inositol contents in tartary buckwheat. *Journal of Agricultural and Food Chemistry, 56*(3), 761–764. https://doi.org/10.1021/jf072453u.
Yang, W., Ma, X., Wang, L., Wei, M., Wang, S., Wu, S., ... Li, Y. (2019). Exploring Chemical Basis of Toxicity Reduction for Processed Roots of Stellera chamaejasme L. Using Ultraperformance Liquid Chromatography-Triple Quadrupole Tandem Mass Spectrometry. *International Journal of Analytical Chemistry, 2019*, 4854728. https://doi.org/10.1155/2019/4854728.
Yang, X., Wei, S., Liu, B., Guo, D., Zheng, B., Feng, L., ... Huang, D. (2018). A novel integrated non-targeted metabolomic analysis reveals significant metabolite variations between different lettuce (Lactuca sativa. L) varieties. *Horticulture Research, 5*, 33. https://doi.org/10.1038/s41438-018-0050-1.
Yao, H., Li, C., Zhao, H., Zhao, J., Chen, H., Bu, T., ... Wu, Q. (2017). Deep sequencing of the transcriptome reveals distinct flavonoid metabolism features of black tartary buckwheat (Fagopyrum tataricum Garetn.). *Progress in Biophysics & Molecular Biology, 124*, 49–60. https://doi.org/10.1016/j.pbiomolbio.2016.11.003.
Zhu, F. (2016). Chemical composition and health effects of Tartary buckwheat. *Food Chemistry, 203*, 231–245. https://doi.org/10.1016/j.foodchem.2016.02.050.